Journal of Luminescence XXXXX

Assessing the interaction of Hecameg® with Bovine Serum Albumin and its effect on protein conformation: A spectroscopic study

J.M. Hierrezuelo[a], B. Nieto-Ortega[b], C. Carnero Ruiz[a]

[a] Department of Applied Physics II, Engineering School, University of Málaga, 29071-Málaga, Spain
[b] Department of Physical Chemistry, Faculty of Sciences, University of Málaga, 29071-Málaga, Spain

abstract

Interaction of the nonionic surfactant Hecameg® with the plasma protein Bovine Serum Albumin (BSA), and its effect on protein conformation, has been studied using spectroscopic techniques such as steady- state and time-resolved fluorescence and circular dichroism. A weak interaction of the surfactant with BSA is reflected by changes in the intrinsic fluorescence of BSA in either steady-state or time-resolved measurements. The fluorescence intensity data allowed us to determine the corresponding binding curve, which suggests a sequential binding mechanism, in which the surfactant first occupies the hydrophobic sites of the inner protein cavity and then, condenses onto the surface hydrophobic sites of BSA via a cooperative mechanism. Additional fluorescence data obtained by synchronous, three- dimensional and anisotropy experiments show that the surfactant mainly interacts with the tryptophan residues of BSA, which seem to experience motional restriction as a result of this interaction. Time- resolved fluorescence data, which were analyzed using the modified Stern–Volmer equation, also support the above mechanism. Finally, far-UV circular dichroism studies indicated that the secondary structure of the protein remains almost unaltered even for BSA to surfactant molar ratio as high as 1 to 100.

1. Introduction

As a result of their numerous uses in a wide variety of biological, industrial, pharmaceutical and cosmetic applications, the interactions between proteins and surfactants have been extensively studied over the past few decades [1–4], especially as the general principles that govern the binding of surfactants to proteins are analogous to those responsible for the stability of other systems such as bilayers, liposomes or biological membranes [5,6]. Consequently, a better understanding of protein-surfactant interactions is essential from both a fundamental point of view and also because it could help us to choose the most appropriate surfactant for a specific application on a rational basis.

It is well-known that ionic surfactants, particularly anionic ones, interact more strongly with proteins than their neutral counterparts and usually cause major conformational changes in their structure [3,4]. As a result, a great deal of experimental effort has been dedicated to characterizing these interactions [7–29]. Although nonionic surfactants have been shown to be less effective protein-binding agents, recent comprehensive studies on the interaction of such surfactants with water-soluble proteins have also been carried out [30–39]. This is mainly due to the fact that the use of nonionic surfactants is preferred for some applications, especially when it is important to preserve protein stability and functionality. There are two areas in which these aspects are of particular relevance: the stability of protein-based pharmaceutical formulations [34–39] and the isolation and purification of membrane proteins [40,41]. In the former, nonionic surfactants are usually added to both liquid and lyophilized formulations to avoid protein destabilization via adsorption or aggregation mechanisms [39]. The study of membrane proteins requires that they are first extracted from the membrane and then maintained in a soluble, native, and functional form. The usual procedure for achieving this involves solubilization of the membrane protein with surfactants, which is one of the most important steps prior to subsequent biochemical and biophysical studies [40,41].

Alkyl polyglycosides (APGs) are by far the most important family of so-called sugar-based surfactants, which are mainly characterized by having a sugar group as the hydrophilic moiety. These surfactants are currently receiving increasing attention as they are produced from renewable sources, exhibit excellent ecological properties, and are nontoxic and dermatologically safe [42–44]. The unique properties of APGs compared with conventional nonionic ethoxylated surfactants make them very useful in the membrane protein field [41], and their possible use for the preparation of pharmaceutical formulations is being evaluated [45]. In light of this, determination of the binding behavior of these surfactants with a model protein is essential as it could provide valuable information regarding the interactions that control this process. With this in mind, we have carried out a spectroscopic study on the interaction between Hecameg® (6-O-(N-heptylcarbamoyl)- methyl-α-D-glucopyranoside) and the water-soluble protein Bovine Serum Albumin (BSA). Hecameg® is an

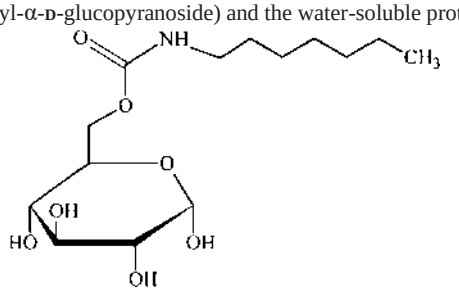

Chart 1. The chemical structure of Hecameg®.

APG surfactant with a well-defined amphiphilic structure (see Chart 1), which has long been considered to be a very mild and effective surfactant for biological applications [46,47] and whose aggregation behavior has been well-characterized [48,49]. BSA, an important transporter binding protein, is probably the most widely used and best characterized protein. The popularity of BSA arises due to its high conformational adaptability to a large variety of ligands, including fatty acids, amino acids, metals drugs, surfactants, etc., thus making it a well-established model protein.

2. Experimental

2.1. Materials

Hecameg® (≥ 99%) was purchased from Fluka and BSA (≥ 98%, agarose gel electrophoresis) was obtained from Sigma-Aldrich. Both products were used as received. All other chemicals were of reagent grade and used without further purification. A 20 mM phosphate buffer of pH 7.4 was prepared in ultra-pure water for all experiments. Stock solutions of Hecameg® and BSA were prepared in aqueous buffer solutions and stored at 4 °C. Working solutions with a fixed protein concentration (15 mM) and different concentrations of surfactant were prepared daily, mixed thoroughly, and stabilized for at least 2 h at 25 °C before any spectroscopic measurement was performed. The ultra-pure water (resistivity ~ 18 MΩ cm^{-1}) used to prepare all the Solutions was obtained by passing pure water from a Millipore Elix system through an ultra-high quality Millipore Synergy purification system.

2.2. Instrumentation and methods

2.2.1. Steady-state fluorescence

All steady-state fluorescence measurements were performed using a FluoroMax-4 (Horiba, Jobin Yvon) spectrofluorometer in "S" mode. Sample solutions were placed in a 1 cm path length quartz cuvette. This apparatus is equipped with a 150-W xenon lamp, a Peltier drive to control the temperature in the cell housing to 25.00 ± 0.05 °C, and a polarization accessory and an automatic interchangeable wheel with Glan-Thompson polarizers. An excitation wavelength of 295 nm was applied to selectively excite the tryptophan residues of BSA, with slit widths of 2 nm and 4 nm for excitation and emission, respectively. The degree of anisotropy (r_{ss}) was determined from the fluorescence polarization experiments, all of which were performed using the same apparatus, as follows

EQ1

where the subscripts of the fluorescence intensity values (I) refer to vertical (V) and horizontal (H) polarizer orientation, and G is the instrumental grating factor required for the L-format configuration [50]. The r_{ss} values were averaged over an integration time of 10 s and a minimum number of three measurements were recorded for each sample.

2.2.2. *Time-resolved* fluorescence

Time-resolved fluorescence measurements were performed using the time-correlated single photon counting technique and a LifeSpec II luminescence spectrometer (Edinburgh Instruments, Ltd.). A nanosecond pulsed light-emitting diode (LED) operating at 295 nm (Edin- burgh Instruments, Ltd.) and a pulse period of 100 ns was employed as the excitation source, with emission being recorded at 349 nm. To optimize the signal-to-noise ratio, 10^4 photon counts were collected in the peak channel. The instrumental response function (IRF) was regularly obtained by measuring the scattering of a Ludox solution. The instrumental full width at half maximum (FWHM) for the 295 nm LED, including the detector response, was about 650 ps. The decay curves were deconvoluted using the FAST software package from Edinburgh Instruments. The intensity decay curves for all lifetime measurements were fitted as a sum of exponential terms:

EQ2

where A_i is a pre-exponential factor for the component i with a lifetime τ_i. In all cases, the best fit was obtained for a biexponential decay curve, where the quality of the fits was determined by the reduced χ^2 values and the distribution of the weighted residuals among the data channels. The statistical criterion determining the goodness of fit was a χ^2 value ≤ 1.20 and a random distribution of weighted residuals. Average fluorescence lifetimes (τ) were calculated from the two-component contributions using the following equation [50]

EQ3

The relative concentration, or fractional amount of each component (α_i), was determined by:

EQ4

2.2.3. *Circular dichroism*

Far-UV circular dichroism (CD) spectra of BSA in the absence and presence of surfactant were recorded using a JASCO 815 spectropolarimeter equipped with a Peltier temperature controller. All CD measurements were performed at 25.0 °C, with a scan speed of 200nmmin^{-1} and a spectral bandwidth of 1 nm. Each spectrum was baseline-corrected, and the final spectrum was taken as the average of five accumulated scans. A dismountable liquid cell with 0.1 cm path length was used, and the spectrometer was continuously purged with dry N_2 gas. For all systems studied, the secondary protein structure was estimated from the corresponding far-UV CD spectrum using the online K2D3 software [51,52].

3. Results and discussion

3.1. *Steady-state fluorescence measurements*

It is well-known that BSA contains two tryptophan residues (Trp-134 and Trp-212). These residues are characteristic of this protein and are chiefly responsible for the intrinsic fluorescence of BSA. The former (Trp-134) is located in the hydrophilic subdomain IB and is thought to be located near the surface of the protein in the second helix of the first domain, whereas the latter (Trp-212) is buried in a hydrophobic pocket in subdomain IIA, which corresponds to the so-called Sudlow I binding site [53].

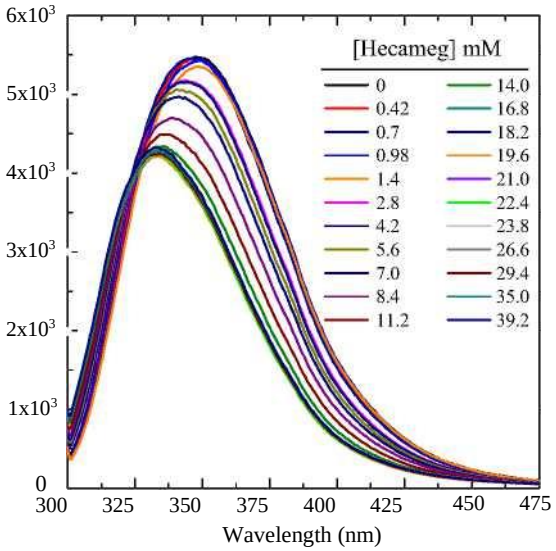

Fig. 1. Emission spectra of BSA (15 mM) with increasing concentrations of Hecamegs in the range from 0 to 39.2 mM at pH 7.4 and 25.0 1C. (2_{exc}_295 nm).

The fluorescence spectrum of BSA in aqueous buffer solutions shows a broad emission band centered at 349 nm when excited at 295 nm (see Fig. 1). The interaction of BSA with surfactants and other ligands is usually accompanied by changes in the emission characteristics of the protein, with modifications in both fluorescence intensity and the position of the emission maximum frequently being observed. As such, the intrinsic fluorescence of BSA can be used to monitor changes in its tertiary structure upon surfactant binding [10]. Fig. 1 shows how the emission spectrum of BSA is affected by surfactant addition. It can be seen from this figure that fluorescence is quenched and the maximum emission wavelength is blue shifted with increasing surfactant concentration, thus suggesting an interaction between the surfactant and the protein. Note that this behavior is similar, although less pronounced, to that previously described in the literature with ionic and non-ionic surfactants [9,10,16,17,26,34–36]. As established above, a band centered at 349 nm, which is clearly associated with native BSA, is observed in the absence of surfactant. The alterations in the BSA emission spectrum at low surfactant concentration (o 1 mM) are minimal, although the fluorescence is steadily quenched with increasing surfactant concentration. The emission maximum also decreases (range: 338–335 nm). Finally, saturation, with an emission maximum located at around 333 nm, is observed above a certain surfactant concentration. Further addition of surfactant does not produce significant alterations in the protein emission spectrum. These spectral changes indicate an interaction between protein and surfactant and reflect the formation of protein-surfactant complexes. However, this binding process only involves conformational changes that do not affect the overall structure of the protein. The blue shift in the emission maxima suggests that the binding of Hecameg® to BSA results in a less polar environment around the fluorophore, that is, the tryptophan residues of BSA, which is usually attributed to the burial of these residues as a result of a more compacted protein [34]. It is important to note that the effect produced by Hecameg® on the emission spectrum of BSA resembles that observed with other nonionic surfactants, such as Triton X-100 [34], MEGA-10 [35], octaethylene-glycol monododecyl ether ($C_{12}E_8$) [36], and Tween 20 and Tween 80 [38], but is less pronounced than that observed for n-octyl-β-D- thioglucoside (OTG), another APG surfactant frequently used in the membrane protein field [36].

Additional insight into the nature of protein-surfactant interactions can be obtained from the so-called binding curve or binding isotherm [54]. This curve can be determined by evaluating the fraction of protein occupied by surfactant, θ, which can be estimated by [15,54]

where I_{obs} is the fluorescence intensity observed at any surfactant concentration, I_0 is the fluorescence intensity in the absence of surfactant, and I_{min} is the minimum fluorescence intensity, that is, the fluorescence intensity under saturation conditions. Fig. 2 shows the change in the intrinsic fluorescence intensity of BSA (I_{obs}) upon surfactant addition. It can be seen that binding of surfactant to BSA induces an initial reduction in fluorescence intensity, and that the fluorescence intensity remains roughly constant (I_{min}) above a certain surfactant concentration, thus indicating that binding saturation occurs. The inset in Fig. 2 shows the binding curve obtained upon plotting the fractional occupation of protein (θ) as a function of total surfactant concentration. It is important to note that the θ parameter does not provide information concerning the average number of surfactant molecules per protein molecule, but rather on the fractional occupation of surfactant binding sites [54]. In other words, if a protein molecule has n_0 binding sites available for a specific surfactant and under certain conditions, the surfactant molecules bind to n sites, the fraction of protein occupied by surfactant is Q_ n/n_0. Thus, in the absence of surfactant I_{obs} _

EQ5

I_0, and Q _ 0. However, saturation is reached when the protein is occupied by the maximum number of surfactant molecules, and in this case I_{obs} _ I_{min}, and Q _ 1. In light of this, our binding curve in Fig. 2 cannot be directly compared with Jones's model [55], which is based on a binding isotherm resulting from plotting the average number of surfactant molecules bound per protein molecule as a function of the logarithm of the free surfactant concentration. However, the analogy of the profiles of both binding curves allows us to draw some conclusions regarding how the binding sites of the protein are occupied by the surfactant. The first part of our binding curve in Fig. 2,at low surfactant concentration, shows that θ increases slightly with surfactant concentration. This behavior can be ascribed to

an initial non-cooperative binding process in which hydrophobic interactions most probably predominate. A sharp increase in θ with total surfactant concentration is observed above a certain surfactant concentration (∈ 3 mM), finally reaching a plateau. This second region clearly reflects a cooperative binding scenario, which finally leads to the saturation binding region.

It has been established previously [3] that the interaction of nonionic surfactants with globular proteins involves the condensation of nonionic surfactants onto non-polar regions of the protein surface. Similar finding have recently been reported by Ruiz-Peña et al. [38], who concluded that the interaction between Tween 20 or Tween 80 and BSA involves more than one mechanism, with the surfactant molecules initially binding to the hydrophobic protein cavity and then interacting with the hydrophobic regions on the protein surface. It is evident that these authors consider that hydrophobic interactions play a predominant role in the binding process. However, some authors have suggested the existence of some type of electrostatic interaction, which contributes favorably to the interactions between nonionic surfactant and BSA [33,34].

It should be noted at this point that previous studies in our laboratory [35,36] showed a more favorable binding of sugar- based surfactants with BSA than that observed with ethoxylated surfactants. This behavior was attributed to the larger critical micelle concentration (CMC) values, which delay the competition between the binding process and micellar formation, and the higher ability of sugar surfactants to form hydrogen bonds between the hydroxyl groups of their hydrophilic head groups and the protein [36]. In the present case, it is evident that both factors are especially favorable for Hecameg®, which contains a high number of hydroxyl groups in its hydrophilic moiety and whose CMC is around 20 mM [48].

The fluorescence observed for BSA in the above steady-state experiments upon excitation at 295 nm was attributed to the tryptophan residues. However, it is well-known that BSA contains three aromatic amino acids, namely tyrosine, tryptophan and phenylalanine, all of which could a priori contribute to the total intrinsic fluorescence of BSA [50]. The contribution of phenylalanine is rather low because is not excited in most experiments and its quantum yield is small [50]. It is well-known that synchronous fluorescence spectra can provide relevant information in multicomponent systems when different wavelength increments, $\Delta\lambda$, are applied, and can also provide information about the local environment in the vicinity of the fluorophore molecule [56]. As such, this spectroscopic technique has been widely used to examine protein-based systems [23–25,56,57]. Synchronous fluorescence spectra were therefore recorded to evaluate the relative contribution of the other residues (tyrosine and tryptophan) in our surfactant-protein system. According to the literature [56], synchronous fluorescence spectra were recorded by applying wavelength increments of 15 nm and 60 nm to determine the contributions of tyrosine and tryptophan residues, respectively. These spectra are displayed in Fig. 3. It can be seen from this figure that the fluorescence intensity of BSA for $\Delta\lambda$ = 60 nm is considerably higher than that for $\Delta\lambda$ = 15 nm, thus indicating that the intrinsic fluorescence of BSA is almost completely produced by the tryptophan residues. It can also be seen that the fluorescence intensity decreases for $\Delta\lambda$ = 60 nm and increases for $\Delta\lambda$ = 15 nm when the surfactant is added. A similar effect has recently been observed for the interaction of different amphiphilic agents with BSA [23,24,57]. Moreover, the data in Fig. 3 also indicate that whereas the fluorescence intensity for $\Delta\lambda$ = 15 nm increases by around 1.5-fold for 5 mM Hecameg® and 2.3-fold for 25 mM Hecameg®,

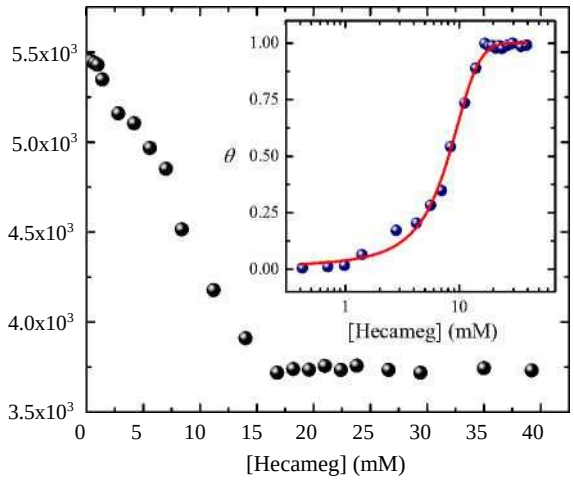

Fig. 2. Intrinsic fluorescence of BSA as a function of the total surfactant concentration in aqueous buffer solutions of pH 7.4 and 25.0 1C. Inset: Binding curve, showing the fraction of a protein molecule bound by surfactant (θ) as a function log of the total surfactant concentration.

an approximately 1.4-fold reduction is observed for AA = 60 nm at both surfactant concentrations. This behavior is probably due to some conformational change produced by the

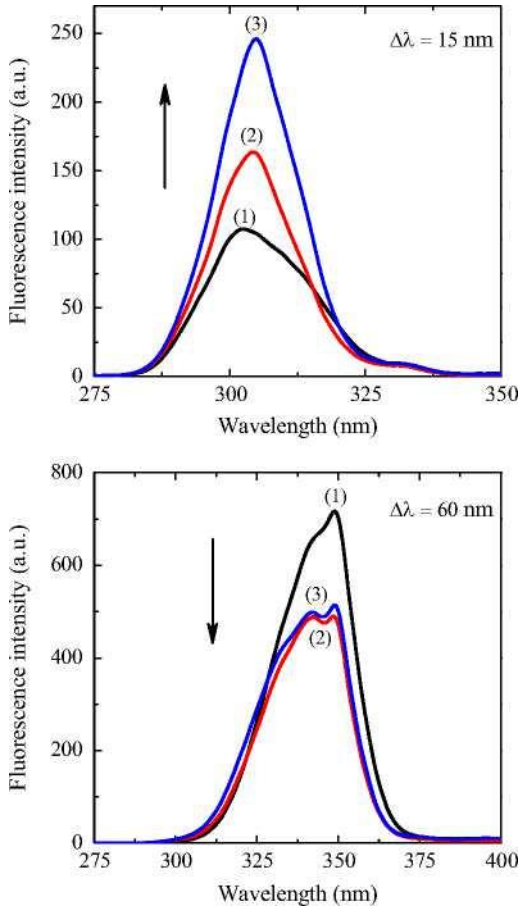

Fig. 3. Synchronous fluorescence spectra of (1) pure BSA, (2) in the presence of 5 mM Hecamegs, and (3) in the presence of 25 mM Hecamegs at AA=15nm (upper panel) and AA=60 nm (bottom panel).

surfactant in the protein, inducing a slight increase in the tyrosine emission and quenching the tryptophan emission. These observations seem to suggest that the surfactant binds in the vicinity of the tryptophan residues at low concentration, thereby quenching the intrinsic fluorescence of BSA. The fact that the presence of additional surfactant molecules does not affect the fluorescence, indicates that the excess of surfactant molecules probably condenses on nonpolar regions of the protein surface, as previously suggested [3,38].

Three-dimensional fluorescence spectroscopy has become a popular analytical technique in recent years as it can provide comprehensive and relevant fluorescence information in complex systems. As such, it has been used to investigate the characteristic conformational changes in protein-based systems [58–61]. Fig. 4 shows the contours of the three-dimensional fluorescence spectra of BSA in buffer solution (Fig. 4A) and in the presence of 25 mM Hecamegs (Fig. 4B). The absence of the first- ($A_{em}=A_{exc}$) and second-order ($A_{em}=2A_{exc}$) Rayleigh scattering peaks, which were masking by the software controlling the spectrofluorometer, should be noted. Fig. 4A shows one peak with a maximum fluorescence intensity of around 6.15 x 10^6 (a.u.) for excitation and emission wavelengths of 289 nm and 349 nm, respectively. As shown in Fig. 4B, this peak was both quenched and blue-shifted upon surfactant addition. In this case, the peak shows a maximum fluorescence intensity of around 4.25 x 10^6 (a.u.) at excitation and emission wavelengths of 289 nm and 333 nm, respectively. Note that these observations are consistent with our results from synchronous fluorescence experiments in the sense that, even when the surfactant is bound to the protein, its intrinsic fluorescence is

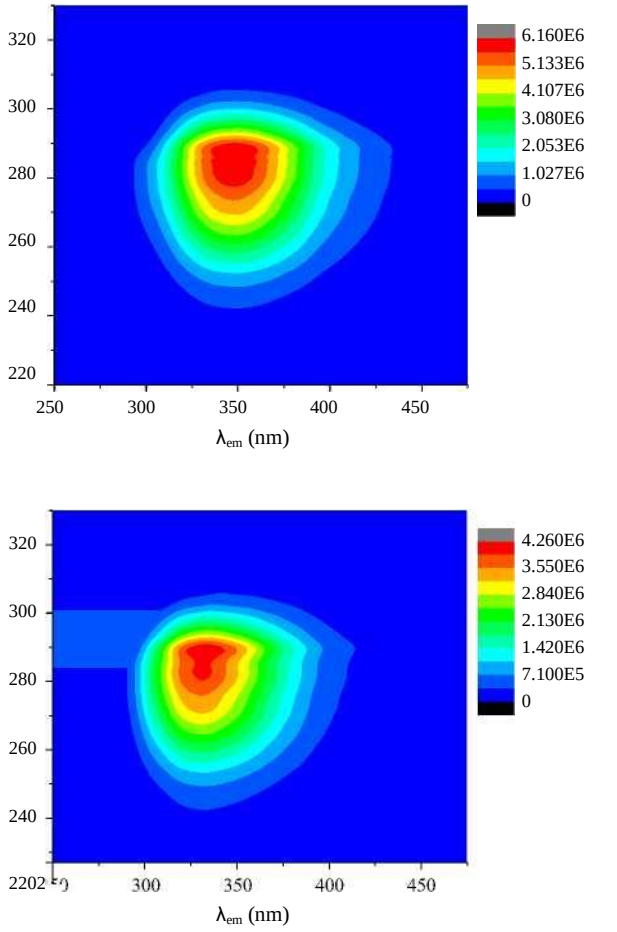

Fig. 4. Contour diagrams of three-dimensional fluorescence spectra of (A) BSA and (B) in the presence of 25 mM Hecameg®. The intensity contours are in arbitrary units as indicated on the scale bars.

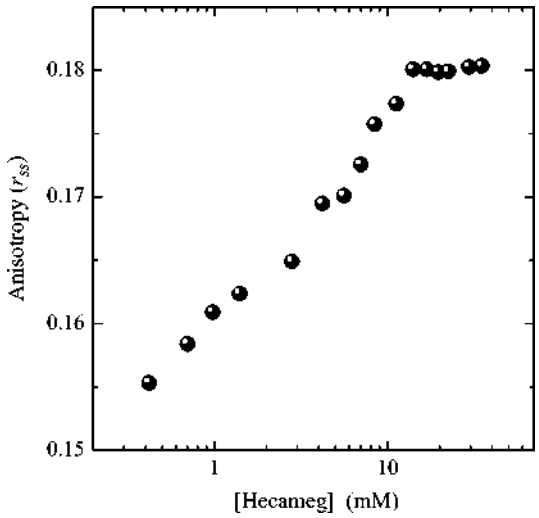

Fig. 5. Fluorescence anisotropy of BSA as a function of the surfactant concentration in aqueous buffer Solutions of pH 7.4 and 25.0 °C (2exc=295 nm, /em —349 nm).

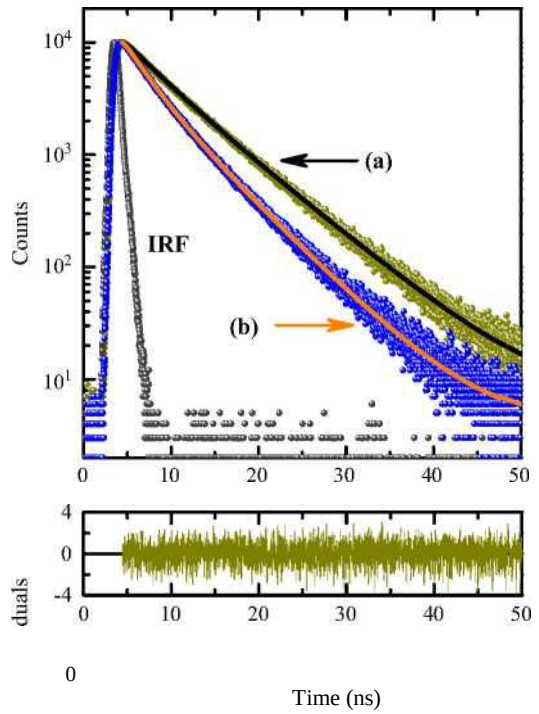

Fig. 6. Typical fluorescence decay curves of BSA (a) pure and (b) in the presence of 18.2 mM Hecameg®, together with the instrumental response function (IRF). The solid line through the data points are the best fits to a double-exponential function. The corresponding weighted residuals are shown in the bottom panels

mainly due to the tryptophan residues. It can be seen that although the tryptophan fluorescence is quenched, these residues nevertheless experience a more hydrophobic environment due to the presence of the surfactant.

With the purpose of gaining additional information about possible conformational changes in the protein as a result of the surfactant binding, polarized fluorescence experiments were performed. Steady-state fluorescence anisotropy measurements of BSA provide information regarding the rotation of the protein molecule as a whole, while the contribution from the rotation of the domain containing the tryptophan residue and the rotation of these groups with respect to the nearby surrounding are considered negligible [62,63]. Fig. 5 shows the results of our steady-state fluorescence anisotropy experiments. Data in Fig. 5 indicate an initial increase in anisotropy values with surfactant concentration and that then levels off. These data seem to indicate a reduction of the rotation diffusion coefficient for the BSA molecule with the surfactant concentration, which can be also explained by the condensation of surfactant molecules onto nonpolar regions of the protein surface, as supported by the other experimental findings.

3.2. Time-resolved fluorescence measurements

We also carried out time-resolved fluorescence studies to gain additional information about the quenching of BSA fluorescence by Hecameg®, as well as the possible structural alterations promoted by surfactant binding. Fig. 6 shows some typical examples of the fluorescence lifetime decay profiles corresponding to pure BSA and in the presence of a certain concentration of Hecameg®. It can also be seen from this figure that the decay curves can be adequately described by double-exponential functions, which is characteristic for tryptophan in proteins [50,64–66]. Table 1 lists the decay parameters of BSA and BSA-

surfactant complexes at some representative surfactant concentrations. It has been postulated that the biexponential decay of tryptophan at neutral pH is due to the existence of three possible rotamers of the indole rings about the C_a- Cp bond within tryptophan [67]. Detailed information on this approach can be found in the literature [64–67]. In short, the so-called "classical rotamer model" establishes that different ground-state conformers of tryptophan, which exist on a longer timescale than the lifetime of the excited state, are subjected to different interactions with other protein residues, thus producing distinct lifetimes [67]. In this manner, when a ligand interacts with a protein, any structural modification of the local tryptophan environment can lead to a distortion of the indole ring planarity, thus stabilizing a particular tryptophan conformation, modifying the distribution of rotamers and altering the lifetime [65,66].

Table 1
Fluorescence lifetime decay analysis of BSA upon Hecameg® addition.

[Surf.] (mM)	τ_1 (ns)	α_1	τ_2 (ns)	α_2	τ (ns)	χ^2
0	2.80	0.24	6.65	0.76	6.20	1.11
0.42	2.59	0.24	6.53	0.76	6.10	1.01
0.98	3.03	0.23	6.52	0.77	6.08	1.03
1.4	2.77	0.23	6.43	0.77	6.02	1.01
4.2	2.73	0.29	6.31	0.71	5.78	1.05
7.0	2.37	0.34	6.15	0.66	5.53	1.03
8.4	2.65	0.42	6.14	0.58	5.31	1.05
11.2	2.47	0.46	5.97	0.54	5.07	1.13
18.2	2.66	0.56	5.71	0.44	4.59	1.13
22.4	2.43	0.52	5.51	0.48	4.50	1.15
26.6	2.39	0.52	5.52	0.48	4.52	1.13
29.4	2.46	0.54	5.57	0.46	4.52	1.17

Turning our attention to the data in Table 1, it can be seen that the two lifetime components for pure BSA in buffer solution (2.80 ns and 6.65 ns) compare well with previously reported values under similar pH conditions [65,66]. It can also be seen that the first component, τ_1, shows only a marginal reduction with increasing surfactant concentration but its contribution increases from 24% to 54%. The second component, τ_2, experiences a more significant reduction but its contribution shows an opposite behavior compared with that of τ_1, decreasing from 76% to 46%. A similar, although more pronounced trend, has recently been observed by Mukherjee and co-workers [26] in their studies of the interaction of the anionic surfactant sodium dodecyl sulfate (SDS) with human serum albumin (HSA). The aforementioned authors [26] also observed that their lifetime data exemplified the stepwise addition of the surfactant in an appropriate manner. The data presented in Table 1 also show the same behavior reflected by the binding curve obtained from steady-state fluorescence measurements (see Fig. 2). Thus, minor changes in lifetime components and contributions are observed at low surfactant concentration (o 1 mM). This first region corresponds to non-cooperative binding between surfactant and protein. The second region, which corresponds to intermediate surfactant concentrations, shows more pronounced changes in both lifetimes and contributions, thus indicating the interaction of significant numbers of surfactant molecules with the protein structure. This region corresponds to the cooperative region in the binding curve. Finally, both lifetimes and contributions are almost constant at high surfactant concentration, thus indicating saturation.

In order to support the aforementioned interaction mechanism, we used a modified Stern–Volmer equation in terms of average lifetime values [26]

$$\log \left(\frac{\tau_0}{\tau} - 1\right) = \log K + n \log [S] \quad (6)$$

where τ_0 and τ are the average lifetime of BSA in the absence and presence of Hecameg®, respectively, K is the binding constant, n the binding affinity, and [S] the surfactant concentration. Fig. 7 shows a plot of our lifetime data according to Eq. (6). It is evident that Fig. 7 shows the same three regions as the inset in Fig. 2, thus indicating the sequential character of Hecameg® binding to BSA.

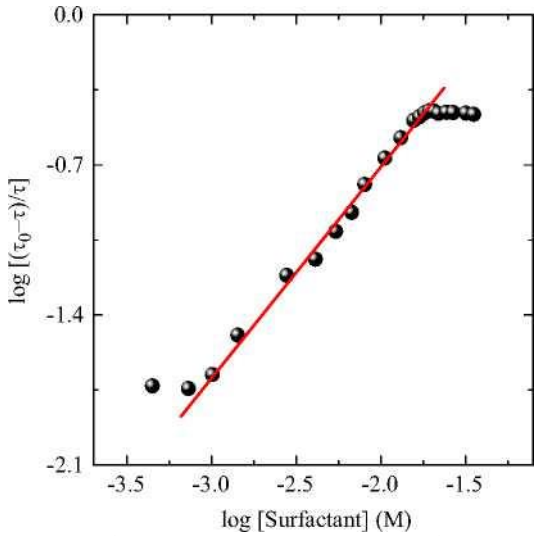

Fig. 7. Modified Stern–Volmer plot for the quenching of BSA by the surfactant. The solid line is the best linear fit of the data, in the intermediate surfactant concentration range, according to Eq. (6).

For comparison purposes, we obtained the values of K and n for our system in the intermediate surfactant concentration range (see Fig. 7). Thus, a linear fitting of our data according to Eq. (6) gave a value of 18.6 L mol^{-1} for *K* and 0.99 for *n*. As expected, this *K* value is small compared to those observed for the interaction of ionic surfactants with different serum albumins [9,10,25,26]. On the other hand, because static and dynamic quenching may be more appropriately distinguished by lifetime measurements, we have used this data to examine the quenching mechanism in our system. Specifically, according

to Mukherjee and co-workers [26,66], we have analyzed the behavior of our average lifetime values (τ). Regarding these values, we can distinguish three different regions. In the first region, from 0 mM to 1.4 mM of surfactant, the average lifetime value is reduced about 3%. In the second region, from 2.8 mM to 18.2 mM, the percentage reduction value is about 21% and, finally, in the saturation region the average lifetime values are almost constants. These data suggest that the mechanism of quenching induced by the surfactant is essentially static in the first and third regions, whereas it is dynamic in nature in the second region.

3.3. *Circular dichroism*

Circular dichroism (CD) has become a powerful spectroscopic tool that has been used to study proteins and other biomolecules since the introduction of the first commercial CD instrumentation in the early 1960s [68]. Far-UV CD spectra, typically in the range 190–240 nm, are determined by the peptide backbone conformation, especially its secondary structure [51,69,70]. As such, it is possible to use such spectra to estimate the secondary structure composition, particularly the contents of the α-helices and extended β-sheets that give rise to the characteristic shape and magnitude of the CD spectrum in the far-UV region [51,68].

CD measurements were carried out to obtain information concerning changes in the secondary structure of BSA upon Hecameg® addition. The CD data were obtained directly in terms of ellipticity (θ_{obs}) and transformed to mean residue ellipticities (MRE in $deg\,cm^{-2}\,dmol^{-1}\,res^{-1}$) using the equation [69]

EQ7

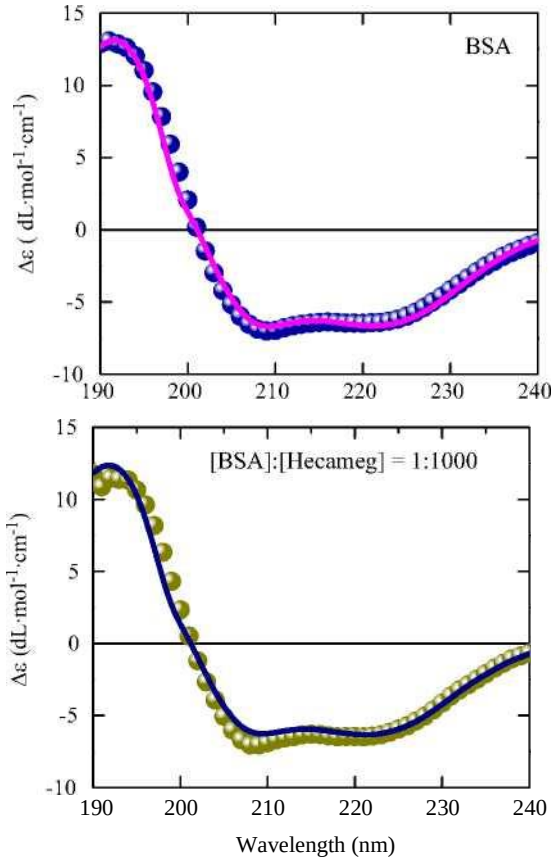

Fig. 8. Far-UV CD spectra of BSA (3 μM) at pH 7.4 and 25.0 1C in the absence of surfactant (upper panel) and in the presence of 3 mM Hecameg® (bottom panel). Scatters represent the experimental data expressed in differential absorption units, Δε, and the solid lines are the corresponding predicted spectra obtained by the online K2D3 software.

Table 2
Contents of α-helix and β-strand of BSA in the absence and presence of Hecameg® at different protein:surfactant molar ratios, at pH 7.4 and 25 1C.

Molar ratio [BSA]:[Surf.]	α-helix (%)	β-strand (%)
1:0	61.0	8.3
1:10	61.5	8.3
1:100	61.3	8.4
1:1000	57.3	9.2

where θ_{obs} is the ellipticity in millidegrees, n is the number of amino acid residues (583 for BSA), c is the protein concentration in mol L 1, and l is the path length of the cell in cm. Finally, the differential extinction coefficients were obtained from [69]

Fig. 8 shows typical far-UV CD spectra for BSA in the absence and presence of 3 mM Hecameg®, with a [BSA]:[Hecameg] molar ratio of 1:1000. A characteristic α-helical protein is described in both cases, with two negative bands centered at around 208 nm and 222 nm and a positive band centered close to 190 nm. No marked changes in the CD spectra of BSA were observed in any of the cases studied. The contents of the secondary structure of BSA

EQ8

were calculated for different molar ratios and are given in Table 2. First of all, it is important to note that the percentage α-helix of BSA in the native form calculated by us is 61%, which is in excellent agreement with the recently reported value (around 60%) under the same experimental conditions (pH 7.4 and 25.0 1C) [59,65,66]. Moreover, the data in Table 2 indicate that the α-helix and β-strand contents remain almost constant up to a molar ratio of 1 to 100, thus indicating that the secondary structure of BSA is practically unaffected by the surfactant. However, the α-helix content decreases to 57.3% and the β-strand content increases to 9.2% at a molar ratio of 1 to 1000. From this marginal change, it is obvious that, even at this molar ratio, the effect of the surfactant on the secondary structure of BSA is rather small.

4. Conclusions

The interaction between the non-ionic surfactant Hecameg® and the protein BSA has been studied by fluorescence and CD techniques. The changes in the intrinsic fluorescence spectra of BSA induced by surfactant addition reveal that the surfactant binds to the protein in a sequential manner. Our data suggest that the surfactant initially interacts with the sites available in the protein hydrophobic cavity and then with the hydrophobic regions on the protein surface by way of a cooperative mechanism. Similar conclusions were reached from the time-resolved fluorescence studies, which also reflect a stepwise

mechanism. Both steady- state and time-resolved fluorescence data indicate that the protein experiences some conformational changes, which do not affect the global structure of the protein, at high surfactant concentrations. Similarly, CD studies indicate that the secondary structure of the protein is not perturbed appreciably upon surfactant binding over the concentration range studied. The results of the present study reflect a weak interaction between surfactant and protein, thus corroborating the mild character of Hecameg®, which justifies its extensive use in the membrane protein field. Furthermore, the present study may stimulate further studies concerning the protective effect of Hecameg® in pharmaceutical formulations, where it could act as a stabilizing agent. Note that the suggested mechanism of saturation of the hydrophobic surface areas could provide steric hindrance, thus reducing the intermolecular con- tacts that lead to the onset of aggregation.

Acknowledgments

This research was financially supported by the "Consejería de Innovación, Ciencia y Empresa de la Junta de Andalucía" (Project P07-FQM-02762). B.N.-O. thanks the Ministerio de Educación (Spain) for her personal grant FPU-AP2009-2797. We thank Prof. F.J. Ramirez for his help with the CD measurements and many stimulating discussions.

References

[1] K.P. Ananthapadmanabhan, Interactions of Surfactants with Polymers and Proteins, in: E.D. Goddard, K.P. Ananthapadmanabhan (Eds.), CRC Press, Boca Raton, FL, 1993. (Chapter 8).
[2] K. Holmberg, B. Jönsson, B. Kronber, B. Lindman, Surfactants and Polymers in Aqueous Solutions, second ed., Wiley, London, 2003.
[3] M.N. Jones, Chem. Soc. Rev. 21 (1992) 127.
[4] D. Otzen, Biochim. Biophys, Acta 2011 (1814) 562.
[5] J.N. Israelachvili, S. Marcelja, R.G. Horn, Q. Rev. Biophys. 13 (1980) 121.
[6] C. Tanford, The Hydrophobic Effect: Formation of Micelles and Biological Membranes, Wiley, New York, 1980.
[7] S.F. Santos, D. Zanette, H. Fischer, R. Itri, J. Colloid Interface Sci. 262 (2003) 400.
[8] N.J. Turro, X.-G. Lei, K.P. Ananthapadmanabhan, M. Aronson, Langmuir 11 (1995) 2525.
[9] E.L. Gelamo, M. Tabak, Spectrochim. Acta, Part A 56 (2000) 2255.
[10] E.L. Gelamo, C.H.T.P. Silva, H. Imasato, M. Tabak, Biochim. Biophys. Acta 1594 (2002) 84.
[11] S. Ghosh, A. Banerjee, Biomacromolecules 3 (2002) 9.
[12] S. Ghosh, Colloids Surf., B 41 (2005) 209.
[13] S. Ghosh, Colloids Surf., B 66 (2008) 178.
[14] T. Chakraborty, I. Chakraborty, S.P. Moulik, S. Ghosh, Langmuir 25 (2009) 3062.
[15] R. Das, D. Guha, S. Mitra, S. Kar, S. Lahiri, S. Mukherjee, J. Phys. Chem. A 101 (1997) 4042.
[16] S. De, A. Girigoswami, S. Das, J. Colloid Interface Sci. 285 (2005) 562.
[17] S. De, S. Das, A. Girigoswami, Colloids Surf., B 54 (2007) 74.
[18] M. Vasilescu, D. Angelescu, M. Almgren, A. Valstar, Langmuir 15 (1999) 2635.
[19] A. Stenstam, A. Khan, H. Wennerström, Langmuir 17 (2001) 7513.
[20] N. Deo, S. Jockusch, N.J. Turro, P. Somasundaram, Langmuir 19 (2003) 5083.
[21] J. Sabín, G. Prieto, A. González-Pérez, J.M. Ruso, F. Sarmiento, Biomacromole- cules 7 (2006) 176.
[22] P. Messina, G. Prieto, V. Dodero, M.A. Cabrerizo-Vílchez, J. Maldonado- Valderrama, J.M. Ruso, F. Sarmiento, Biopolymers 82 (2006) 261.
[23] D. Wu, G. Xu, Y. Sun, H. Zhang, H. Mao, Y. Feng, Biomacromolecules 8 (2007) 708.
[24] D. Wu, G. Xu, Y. Sun, Y. Feng, Y. Wang, Y. Zhu, Colloid Polym. Sci. 287 (2009) 225.
[25] T. Zhou, M. Ao, G. Xu, T. Liu, J. Zhang, J. Colloid Interface Sci. 389 (2013) 175.
[26] U. Anand, C. Jash, S. Mukherjee, J. Phys. Chem. B 114 (2010) 15839.
[27] P.P. Misra, N. Kishore, J. Colloid Interface Sci. 354 (2011) 234.
[28] S. Tu, X. Jiang, L. Zhou, W. Yin, H. Wang, M. Duan, P. Liu, X. Jiang, J. Lumin. 132 (2012) 371.
[29] Y. Moriyama, N. Kondo, K. Takeda, Langmuir 28 (2012) 16268.
[30] W.W. Sukow, H.S. Sanderg, E.A. Lewis, D.J. Eatough, L.D. Hansen, Biochemistry 19 (1980) 912.
[31] T. Cserháti, Environ. Health Perspect. 103 (1995) 358.
[32] A.D. Nielsen, K. Borch, P. Westh, Biochim. Biophys. Acta 1479 (2000) 321.
[33] U. Kragh-Hansen, F. Hellec, B. de Foresta, M. le Marie, J.V. Moller, Biophys. J. 80 (2001) 2898.
[34] K.S. Singh, N. Kishore, J. Phys. Chem. B 110 (2006) 9728.
[35] C. Carnero Ruiz, J.M. Hierrezuelo, J. Aguiar, J.M. Peula-García, Biomacromole- cules 8 (2007) 2497.
[36] C. Carnero Ruiz, J.M. Hierrezuelo, J.M. Peula-García, J. Aguiar, Sugar-Based Surfactants: Fundamentals and Applications, in: C. Carnero Ruiz (Ed.), CRC Press, Boca Raton, 2009. (Chapter 14).
[37] W.J. Mcauley, D.S. Jones, V.L. Kett, J. Pharm. Sci. 98 (2009) 2659.
[38] M. Ruiz-Peña, R. Oropesa-Nuñez, T. Pons, S.R.W. Louro, A. Pérez-Gramatges, Colloids Surf., B 75 (2010) 282.
[39] E.Y. Chi, S. Krishnan, T.W. Randolph, J.F. Carpenter, Pharm. Res. 20 (2003) 1325.
[40] R.M. Garavito, S. Ferguson-Miller, J. Biol. Chem. 276 (2001) 32403.
[41] T. Arnold, D. Linke, Biotechniques 43 (2007) 427.
[42] M.T. García, I. Ribosa, E. Campos, J. Sánchez Leal, Chemosphere 35 (1997) 545.
[43] W. von Rybinski, K. Hill, Angew. Chem. Int. Ed. 37 (1998) 1328.
[44] O. Söderman, I. Johansson, Curr. Opin. Colloid Interface Sci. 4 (2000) 391.
[45] E. Söderlind, M. Wollbratt, C. von Corswant, Int. J. Pharm. 252 (2003) 61.
[46] D. Plusquellec, G. Chevalier, R. Talibart, H. Wróblewski, Anal. Biochem. 179 (1989) 145.
[47] M.B. Ruiz, A. Prado, F.M. Goñi, A. Alonso, Biochim. Biophys, Acta 1193 (1994) 301.
[48] M. Frindi, B. Michels, R. Zana, J. Phys. Chem. 96 (1992) 8137.
[49] M. Aoudia, R. Zana, J. Colloid Interface Sci. 206 (1998) 158.
[50] J.R. Lakowicz, Principles of Fluorescence Spectroscopy, third ed., Springer, New York, 2006.
[51] C. Louis-Jeune, M.A. Andrade-Navarro, C. Perez-Iratxeta, Proteins 80 (2012) 374.
[52] ⟨http://www.ogic.ca/projects/k2d3/⟩.
[53] T. Peters Jr, All About Albumin, Academic Press, San Diego, C.A, 1996.
[54] J.M. Andreu, J.M. Muñoz, Biochemistry 25 (1986) 5220.
[55] M.N. Jones, Biochem. J. 19 (1975) 109.
[56] D. Patra, C. Barakat, R.M. Tafech, Colloids Surf., B 94 (2012) 354.
[57] X. Wang, J. Liu, L. Sun, L. Yu, J. Jiao, R Wang, J. Phys. Chem. B 116 (2012) 12479.
[58] Y. Shu, M. Liu, S. Chen, X. Chen, J. Wang, J. Phys. Chem. B 115 (2011) 12306.
[59] F.-F. Tian, F.-L. Jiang, X.-L. Han, C. Xiang, Y.-S. Ge, J.-H. Li, Y. Zhang, R. Li, X.- L. Ding, Y. Liu, J. Phys. Chem. B 114 (2010) 14842.
[60] L. He, X. Wang, B. Liu, J. Wang, Y. Sun, E. Gao, S. Xu, J. Lumin. 131 (2011) 285.

[61] X. Shi, X. Li, M. Gui, H. Zhou, R. Yang, H. Zhang, Y. Jin, J. Lumin 130 (2010) 637.
[62] P. Mandal, T. Ganguly, J. Phys. Chem. B 113 (2009) 14904.
[63] B. Ojha, G. Das, J. Phys. Chem. B 114 (2010) 3979.
[64] J.A. Ross, D.M. Jameson, Photochem. Photobiol. Sci. 7 (2008) 1301.
[65] U. Anand, C. Jash, R.K. Boddepalli, A. Shrivastava, S. Mukherjee, J. Phys. Chem. B 115 (2011) 6312.
[66] U. Anand, L. Kurup, S. Mukherjee, Phys. Chem. Chem. Phys. 14 (2012) 4250.
[67] A.G. Szabo, D.M. Rayner, J. Am. Chem. Soc. 102 (1980) 554.
[68] N. Sreerama, R.W. Woody, Circular dichroism, in: E.D. Nakanishi, K. Berova, N. Woody, R.W. (Eds.), Principles and Applications, VCH Publishers Inc, New York, 2000. (Chapter 21).
[69] S.M. Kelly, T.J. Jess, N.C. Price, Biochim. Biophys. Acta 1751 (2005) 119.
[70] W. Moffitt, J. Phys. Chem. 25 (1956) 467.